

# A MULTISCALE MODEL FOR THE ELASTIC MODULUS OF CERAMSITE LIGHTWEIGHT AGGREGATE CONCRETE AFTER ELEVATED TEMPERATURES

JIANMIN WANG<sup>1\*</sup>, CHENGFENG ZHU<sup>1</sup>, BO CHENG<sup>1,2</sup>, JUNZHE LIU<sup>1</sup>

<sup>1</sup>School of Civil and Environmental Engineering, Ningbo University, Ningbo 315211, China

<sup>2</sup>Ningbo Huacong Architectural Design & Research Institute Co., LTD, Ningbo 315010, China

*The elastic modulus of ceramsite lightweight aggregate concrete (LWAC) after elevated temperatures is studied and modeled in this work. The degeneration for the effective stiffness contribution by ceramsite aggregates to LWAC together with the phase transformations of hardened cement paste are considered. Five levels, room temperature (20°C), 200°C, 400°C, 600°C and 800°C, are selected to conduct the elevated temperature experiment. For the phase-change analysis at the cement paste level, the mass loss of test blocks after drying at 120°C is obtained to further validate the initial volume fraction of the remaining water, the capillary voids and the water in gels in the cement paste. The experimental damage characteristics of ceramsite LWAC after elevated temperatures indicate a reduction in the effective stiffness contribution of ceramsite aggregates to LWAC. The effective elastic modulus  $E'_a$  of ceramsite aggregates in LWAC and the nominal elastic modulus  $E_a$  of the ceramsite particle are utilized to formulate the degradation model for the stiffness contribution of ceramsite aggregates to LWAC after elevated temperatures. The proposed polyline reduction model effectively characterizes the variation trend of the elastic modulus of LWAC after elevated temperatures.*

**Keywords:** Lightweight aggregate concrete; Elastic modulus; Ceramsite; Elevated temperature; Model.

## 1. Introduction

The strength and stiffness of concrete will decrease as exposing to high temperature. As a kind of complicated composite material with a variety of heterogeneities, concrete can be regarded as homogeneous at the macroscopic level. But at the mesoscopic level, it is treated as consisting of coarse aggregates and mortar matrix. Further subdivisions of the mortar matrix produce fine aggregates and hardened cement paste with pores embedded inside [1]. The multiscale approach was proposed including four scale levels for concrete from the smallest characteristic length scale to the macroscopic level [2]:

(I) Level I (the C-S-H level,  $10^{-8}\sim 10^{-6}$  m): At least two types (inner and outer) of Calcium-Silicate-Hydrate (C-S-H) exist with different volume fractions;

(II) Level II (the cement paste level,  $10^{-6}\sim 10^{-4}$ m): Homogeneous C-S-H with large  $\text{Ca}(\text{OH})_2$  crystals, aluminates, cement clinker inclusions, water and some capillary porosity depending on the water/cement ratio;

(III) Level III (the mortar level,  $10^{-3}\sim 10^{-2}$ m): A three-phase composite material composed of a cement paste matrix, sand particle inclusions, and an interfacial transition zone (ITZ).

(IV) Level IV (the concrete level,  $10^{-2}\sim 10^{-1}$ m): A three-phase material composed of coarse aggregates embedded in a homogeneous mortar matrix and an ITZ.

Compared with the normal weight aggregate

concrete (NWAC), ceramsite lightweight aggregate concrete (LWAC) shows a better thermal stability as ceramsite aggregate is made by high temperature sintering, which generates more internal holes inside the aggregate [3]. It was pointed out that NWAC with siliceous aggregates shows significant strength loss as temperature approximately exceeds 430°C compared with LWAC [4]. LWAC can preserve its strength up to nearly 500°C, and the residual strength after fire linearly decreases from 100% to 40% as temperature increasing from 500°C to 800°C [5,6]. Lee et al. proposed a multiscale chemo-mechanical model for the thermal degradation of elastic modulus of NWAC based on composite mechanics [7], in which the temperature dependence of fine and coarse aggregates was expressed by unified thermal degeneration factor.

In fact, aggregate plays an important role on the degradation of concrete in high temperature. It was concluded that when elastic moduli of the two kinds of components are close, the composite material under the constant stress and strain mode assumption becomes more acceptable [8]. The elastic modulus of lightweight aggregates is compatible with that of cement paste, which reduces the tendency for the ITZ microcracking in LWAC [9]. At the same time, significant differences exist in the mechanical/thermal performance between the ceramsite aggregates in LWAC and the conventional coarse aggregate (CCA) in NWAC such as granitic gravels. Therefore, the ceramsite coarse aggregates and the conventional fine aggregates are considered independently to study

\* Autor corespondent/Corresponding author,  
E-mail: [wangjianmin@nbu.edu.cn](mailto:wangjianmin@nbu.edu.cn)

the degradation of elastic modulus of LWAC after elevated temperatures by the multiscale modelling method.

## 2. Phase-change at the cement paste level

### 2.1. Normal temperature state

The initial volume fractions of constituents in the cement paste are important to analyze the phase transformation as exposed to high temperature. In this paper, the calculation method of initial volume fractions for LWAC constituents at the cement paste level refers to that of NWAC [7,10]. The total volume at the cement paste level is composed of reactants (remaining water and cement grains) and products of hydration reaction (C-S-H, CH, aluminates products and capillary voids), which is expressed as following,

$$V_{\text{Cem}}^{\text{Tot}} = V_w(t) + \sum_i V_i^{\text{Re}}(t) + V_{\text{C-S-H}}(t) + V_{\text{CH}}(t) + V_{\text{AL}}(t) + V_{\text{Void\_C}}(t) = V_w^0 + V_c^0 \quad (1)$$

where  $t$  is the characteristic hydration time;

$V_i^{\text{Re}}(t)$  — the remaining cement volume including  $\text{C}_3\text{S}$ ,  $\text{C}_2\text{S}$ ,  $\text{C}_3\text{A}$ ,  $\text{C}_4\text{AF}$  and other impurity things;

$V_{\text{C-S-H}}$ ,  $V_{\text{CH}}$  — the volumes of hydration products from  $\text{C}_3\text{S}$  and  $\text{C}_2\text{S}$  respectively;

$V_{\text{AL}}(t)$ ,  $V_{\text{Void\_C}}(t)$  —volumes of aluminum hydrates, the capillary voids from chemical shrinkage of hydration.

$V_w(t)$  is the volume of remaining water after hydration reaction, which is determined by subtracting the water during hydration reaction from the initial water volume  $V_w^0$  as,

$$V_w(t) = V_w^0 - \sum_i V_i^j \times \alpha_i(t) \quad (2)$$

in which,  $V_i^j$  is the water volume consumed for complete hydration of clinker  $i$ , it is obtained by,

$$\frac{V_i^j}{V_c^0} = N_i^j \times \frac{\rho_i^* / \mu_i}{\rho_w / \mu_w}, \rho_i^* = \frac{M_i}{V_c^0} = \rho_c \frac{m_i}{\sum_i m_i} \quad (3)$$

where  $V_c^0$  is the initial volume of the cement;

$m_i$  — the mass of each clinker phase ( $\text{C}_3\text{S}$ ,  $\text{C}_2\text{S}$ ,  $\text{C}_3\text{A}$ ,  $\text{C}_4\text{AF}$ ) in the cement;

$\mu_i$  — the molar mass of phase  $i$ ;

$N_w^j = n_w / n_i$  — moles of consumed water for  $n_i=1$  mol of phase  $i$  during hydration;

$\alpha_i(t)$  — the hydration degree of the clinker phase  $i$ .

$V_i^{\text{Re}}(t)$  is calculated from Eq.(4),

$$V_i^{\text{Re}}(t) = V_i^{\text{Re}_0} [1 - \alpha_i(t)] \quad (4)$$

in which,  $V_i^{\text{Re}_0}$  is the initial volume of the clinker phases in the cement.

$V_{\text{C-S-H}}(t)$  and  $V_{\text{CH}}(t)$  are determined by,

$$\begin{aligned} V_{\text{C-S-H}}(t) &= V_{\text{C-S-H}}^{\text{C}_3\text{S}} \times \alpha_{\text{C}_3\text{S}}(t) + V_{\text{C-S-H}}^{\text{C}_2\text{S}} \times \alpha_{\text{C}_2\text{S}}(t), \\ V_{\text{CH}}(t) &= V_{\text{CH}}^{\text{C}_3\text{S}} \times \alpha_{\text{C}_3\text{S}}(t) + V_{\text{CH}}^{\text{C}_2\text{S}} \times \alpha_{\text{C}_2\text{S}}(t) \end{aligned} \quad (5)$$

$V_{\text{C-S-H}}^{\text{C}_3\text{S}}$ ,  $V_{\text{C-S-H}}^{\text{C}_2\text{S}}$  — volumes of reaction products C-S-H from hydration reaction of  $\text{C}_3\text{S}$  and  $\text{C}_2\text{S}$  respectively;

$V_{\text{CH}}^{\text{C}_3\text{S}}$ ,  $V_{\text{CH}}^{\text{C}_2\text{S}}$  — volumes of reaction products CH from hydration reaction of  $\text{C}_3\text{S}$  and  $\text{C}_2\text{S}$  respectively.

They are determined by Eq.(6) and Eq.(7).

$$\begin{aligned} \frac{V_{\text{C-S-H}}^{\text{C}_3\text{S}}}{V_c^0} &= N_{\text{C-S-H}}^{\text{C}_3\text{S}} \times \frac{\rho_{\text{C}_3\text{S}}^* / \mu_{\text{C}_3\text{S}}}{\rho_{\text{C-S-H}} / \mu_{\text{C-S-H}}}, \rho_{\text{C}_3\text{S}}^* = \frac{M_{\text{C}_3\text{S}}}{V_c^0} = \rho_c \frac{m_{\text{C}_3\text{S}}}{\sum_i m_i}, \\ \frac{V_{\text{C-S-H}}^{\text{C}_2\text{S}}}{V_c^0} &= N_{\text{C-S-H}}^{\text{C}_2\text{S}} \times \frac{\rho_{\text{C}_2\text{S}}^* / \mu_{\text{C}_2\text{S}}}{\rho_{\text{C-S-H}} / \mu_{\text{C-S-H}}}, \rho_{\text{C}_2\text{S}}^* = \frac{M_{\text{C}_2\text{S}}}{V_c^0} = \rho_c \frac{m_{\text{C}_2\text{S}}}{\sum_i m_i} \end{aligned} \quad (6)$$

$$\frac{V_{\text{CH}}^{\text{C}_3\text{S}}}{V_c^0} = N_{\text{CH}}^{\text{C}_3\text{S}} \times \frac{\rho_{\text{C}_3\text{S}}^* / \mu_{\text{C}_3\text{S}}}{\rho_{\text{CH}} / \mu_{\text{CH}}}, \frac{V_{\text{CH}}^{\text{C}_2\text{S}}}{V_c^0} = N_{\text{CH}}^{\text{C}_2\text{S}} \times \frac{\rho_{\text{C}_2\text{S}}^* / \mu_{\text{C}_2\text{S}}}{\rho_{\text{CH}} / \mu_{\text{CH}}} \quad (7)$$

$N_{\text{C-S-H}}^{\text{C}_3\text{S}}$ ,  $N_{\text{C-S-H}}^{\text{C}_2\text{S}}$  — moles of hydration products C-S-H from 1 mol of  $\text{C}_3\text{S}$  and  $\text{C}_2\text{S}$  respectively;

$N_{\text{CH}}^{\text{C}_3\text{S}}$ ,  $N_{\text{CH}}^{\text{C}_2\text{S}}$  — moles of hydration products CH from 1 mol of  $\text{C}_3\text{S}$  and  $\text{C}_2\text{S}$  respectively;

$\rho_{\text{C}_3\text{S}}^*$  ( $\rho_{\text{C}_2\text{S}}^*$ ) — the apparent mass density of  $\text{C}_3\text{S}$  ( $\text{C}_2\text{S}$ ) in cement (mass density is  $\rho_c$ );

$\mu_{\text{C}_3\text{S}}$  ( $\mu_{\text{C}_2\text{S}}$ ) — the molar mass of  $\text{C}_3\text{S}$  ( $\text{C}_2\text{S}$ ).

Therefore,  $\rho_{\text{C}_3\text{S}}^* / \mu_{\text{C}_3\text{S}}$  denotes the moles of  $\text{C}_3\text{S}$  per unit volume of cement; and  $\rho_{\text{C-S-H}} / \mu_{\text{C-S-H}}$  is moles of C-S-H per unit volume of C-S-H.

The concrete parameters used in aforementioned equations are listed in Table 1 [10]. The hydration reaction formulas comes from Lee and Bernard et al. [7,10].

The capillary voids due to the chemical shrinkage during hydration reaction may be approximated as following [11],

$$V_{\text{Void\_C}}(t) = C_s \times \rho_c \times V_c^0 \times \alpha(t) \quad (8)$$

$C_s$  represents the chemical shrinkage per gram of cement which is suggested to take as 0.07 ml/g [10]. All volume fractions can be expressed respectively as following,

$$f_i = \frac{V_i}{V_{\text{M}}^{\text{Tot}}} = \frac{V_i}{V_w^0 + V_c^0} = \frac{V_i}{V_c^0} \left(1 + \frac{\rho_c}{\rho_w} \times \frac{w}{c}\right) \quad (9)$$

$V_{\text{M}}^{\text{Tot}}$  is the total volume of cement and water in the mixture. The volume fraction of aluminates is evaluated by,

$$f_{\text{AL}} = \frac{V_{\text{AL}}}{V_{\text{M}}^{\text{Tot}}} = 1 - (f_w + \sum_i f_i^{\text{Re}} + f_{\text{C-S-H}} + f_{\text{CH}} + f_{\text{Void\_C}}) \quad (10)$$

Table 1

Parameters	Reactants						Products		
	C <sub>3</sub> S	C <sub>2</sub> S	C <sub>3</sub> A	C <sub>4</sub> AF	w	Cement	C <sub>3,4</sub> S <sub>2</sub> H <sub>8</sub>	(C <sub>3,4</sub> S <sub>2</sub> H <sub>3</sub> )	CH
$\rho_i^*$ [g/cm <sup>3</sup> ]	$\rho_{C_3S}^*$	$\rho_{C_2S}^*$	$\rho_{C_3A}^*$	$\rho_{C_4AF}^*$	1.00	3.15	2.04	1.75	2.24
$\mu_i$ [g/mol]	228.32	172.24	270.20	430.12	18	-	227.2	365	74
$N_{C-S-H}$	1.0	1.0	-	-	-	-	-	-	-
$N_{CH}$	1.3	0.3	-	-	-	-	-	-	-
$N_w$	5.3	4.3	10.0	10.75	-	-	-	-	-

## 2.2. Elevated temperature state

Physical and chemical variations take place in concrete as exposed to high temperature. The remaining free water (including water in gel pores) firstly completely evaporates at about 120°C [12]. The loss of the chemically bounding water in C-S-H starts at 150°C and reaches a peak loss rate at 270°C [13]. The propagation of micro-cracks occurs at 300°C, and the mechanical strength and thermal conductivity are degraded at this stage with possible associated expansion [14]. Between 400°C~600°C, complete desiccation and decomposition of crystals of calcium hydroxide into their original components (CaO and water) further weaken the concrete [15]. C-S-H decomposes continually above 600°C, and the cement paste transforms into a glass phase above 1150°C.

The exact formulation on each phase transformation process exposed to elevated temperature is difficult. Thus, the following hypotheses are necessary at present for further analysis:

(1) Cement paste expands above 150°C and the maximum expansion ratio is 0.2%; the hardened cement paste shrinks from 300°C to 800°C, and the shrinkage is between 1.6% and 2.2% at 800°C. This is quite smaller than the initial total volume, so the total volume of hardened cement paste may be assumed as constant.

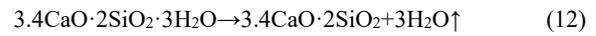
(2) Assuming the phase transformation progress linearly from the beginning to end, and the volume fractions of the constituents are linear functions about the temperature in the model.

(3) For the trivial influence on the concrete stiffness, the aluminum hydrates are regarded as non-reactive substances independent of the temperature variation.

Supposing the total initial void fraction at the cement level approximately equals to the sum of the remaining water volume, the capillary void and the volume of water in gel pores,

$$V_{\text{Void}} = f_w + f_{\text{Void,C}} + f_{w,G} \quad (11)$$

$f_{w,G}$  is about 28% that of C-S-H gel [16]. After evaporation of free water in gel pores, the chemical formula of C-S-H changes into C<sub>3,4</sub>-S<sub>2</sub>-H<sub>3</sub> [17]. It means that five moles of H<sub>2</sub>O (free water in gel pores) per unit mol of C-S-H evaporate between 100°C and 120°C. The decomposition of C-S-H is expressed as,



The decomposition of CH between 400°C and 530°C follows as,



Volumes of CaO decomposed from CH and C<sub>34</sub>S<sub>2</sub> decomposed from C<sub>34</sub>S<sub>2</sub>H<sub>3</sub> are calculated by reducing the decomposed water volume from initial volumes of CH and C<sub>34</sub>S<sub>2</sub>H<sub>3</sub>. Different decomposition processes with respect to different temperature ranges obtained from literatures are listed in Table 2 [7].

It is assumed that CH and C-S-H completely decomposes above 530°C and 800°C levels respectively. The volume of water decomposed from C-S-H and CH is regarded as additional voids generating. Therefore, the volume fraction of the total water decomposed from C-S-H (between 120°C and 800°C) and CH (between 400°C and 530°C) is calculated from Eq.(14),

$$f_i^w = f_i \times N_w^i \times \frac{\rho_i^* / \mu_i}{\rho_w / \mu_w}, (i = \text{C-S-H, CH}) \quad (14)$$

$N_w^i = n_w / n_i$  equals to 3.0 and 1.0 respectively for C-S-H and CH, which means that  $N_w$  moles of water is decomposed from 1 mol of phase  $i$  ( $N_w^{\text{C-S-H}}=3.0$ ,  $N_w^{\text{CH}}=1.0$ ).

Table 2

Temperature	Decomposition
100°C~120°C	Evaporation of free water, dehydration of C-S-H and ettringite
120°C~400°C	Dehydration of C-S-H
400°C~530°C	Dehydration of C-S-H and CH
530°C~600°C	Dehydration of C-S-H, decomposition of poorly crystallized CaCO <sub>3</sub>
600°C~800°C	Dehydration of C-S-H, decomposition of CaCO <sub>3</sub>

Table 3

**Clinker composition of the cement**

Clinker phases	C <sub>3</sub> S	C <sub>2</sub> S	C <sub>3</sub> A	C <sub>4</sub> AF	Free-CaO	Loss of ignition
Mass fraction (%)	60.2	17.2	7.7	12.92	0.95	1.03

Table 4

**Mixture composition of LWAC**

Mixture	Cement	Water	River sands	Ceramsite
(kg/m <sup>3</sup> )	460	210	500	780
Volume fraction	Cement paste ( <i>f<sub>c</sub></i> )		Sand ( <i>f<sub>s</sub></i> )	Ceramsite ( <i>f<sub>m</sub></i> )
(%)	34.219		18.483	47.298

Table 5

**Mass loss of cubic test blocks after elevated temperatures**

		Referring state 20°C / ( <i>m<sub>0</sub></i> )	Drying state 120°C ( <i>m<sub>D</sub></i> )	200°C ( <i>m<sub>200</sub></i> )	400°C ( <i>m<sub>400</sub></i> )	600°C ( <i>m<sub>600</sub></i> )	800°C ( <i>m<sub>800</sub></i> )
Mass (g)		1847	1772	1670	1647	1637	1613
		-	<i>m<sub>D</sub></i> - <i>m<sub>0</sub></i>	<i>m<sub>200</sub></i> - <i>m<sub>D</sub></i>	<i>m<sub>400</sub></i> - <i>m<sub>D</sub></i>	<i>m<sub>600</sub></i> - <i>m<sub>D</sub></i>	<i>m<sub>800</sub></i> - <i>m<sub>D</sub></i>
Variation	(g)	-	-75	-102	-125	-135	-159
	(%)*	-	21.92				
Calculated model ( <i>f<sub>Void_C</sub></i> + <i>f<sub>w</sub></i> + <i>f<sub>Void_G</sub></i> )	(%)	-	25.20				

\* It is the ratio for the volume of the mass variation from water evaporation to that of cement paste.

### 2.3. Experimental verification

The pore volume variation after elevated temperatures is used to validate the aforementioned model and is compared with the theoretical calculation on the porosity change [18]. In this study, the mass variation of LWAC is used for comparing with the presented model. The stacking and apparent densities of the ceramsite aggregate are 915 kg/m<sup>3</sup> and 1585 kg/m<sup>3</sup> respectively. The water absorption ratio after 24 hours soaking is about 8% to 12%. The composition of clinker phases in the cement is listed in Table 3.

The mixture composition of LWAC is listed in Table 4. 100×100×100 mm and 100×100×300 mm test blocks were made. Elevated temperature of 200°C, 400°C, 600°C and 800°C were selected for the experiment. Test blocks were pre-dried in the oven at 120 °C for 24 hours before heating. One of the purposes is to estimate the volume fractions of the remaining water and water in gel pores in the blocks according to the mass loss; the other is to avoid the spall happening during heating. Test blocks were naturally air-cooled after elevated temperatures. The mass variation after experiment is listed in Table 5.

The referring state (20°C) in Table 5 is that test blocks were taken out after 28 days of standard curing saturated in water. It is assumed that, from the referring state to that after drying at 120 °C level, the average mass loss is due to the evaporation of the remaining water, the free water in capillary voids and the water in gel pores in the cement paste of LWAC, and they are assumed fully evaporating [7,14]. The volume fraction calculated according to the mass loss from experiment is 21.92%, which is a little lower than

that from the proposed model. Maybe there are some capillary voids in cement paste that are closed without water in them in the referring state.

The mass reduction of the cement paste calculated from the model because of the water evaporation decomposed from C<sub>3,4</sub>S<sub>2</sub>H<sub>3</sub> and CH after 800°C high temperature is 66.9 grams. The total mass reduction of test blocks after 800°C corresponding to the drying state at 120°C is 159 grams, possibly because it includes the ignition loss of impurity things in the blocks.

### 3. Reduction model of the elastic modulus of LWAC

Phase transformations take place in concrete under high temperature. Some phases with higher moduli are converted into other phases with lower moduli or even with zero moduli (such as voids). Lee et al. introduced the theory of composite damage mechanics into the phase transformation on the stiffness of concrete [7]. As a kind of composite material, the elastic modulus of the cement paste after the phase transformation can be expressed based on the composite damage mechanics [19,20],

$$E_e^T = (f_{C_{3,4}S_2H_3}^T \cdot f_{CH}^T \cdots) \cdot E_{Ref} = (\prod_{j=C_{3,4}S_2H_3}^N f_j^T) \cdot E_{Ref} \quad (15)$$

$E_{Ref}$  is the initial elastic modulus.  $f_j^T$  is the temperature dependence factor of the elastic modulus for each phase from the original to the decomposed state during phase transformation. For a composite with new and original phases, if new phases randomly distribute among original phases with spherical shapes and different sizes, the temperature dependence factor is expressed as,

$$f_j^r(c_2) = 1 + \frac{c_2}{(1-c_2)/3 + 1/[(E_2/E_1) - 1]} \quad (16)$$

In which,  $E_2$ ,  $E_1$  — moduli of the new phase and the original respectively;

$C_2$  — the volume fraction of the new phase product.

### 3.1. Thermal degradation of ceramsite aggregates of LWAC

When the elastic moduli of two components are close, the composite material under the constant stress/strain state assumption becomes more acceptable [8]. There is more obvious difference on the strength/stiffness between ceramsite coarse aggregates and the mortar in LWAC than that in NWAC. The elastic modulus of a single particle of ceramsite aggregate  $E_a$  can't accurately represent the actual contribution of the ceramsite aggregate in LWAC under loading. The more rational representation is the effective elastic modulus of ceramsite aggregates  $E'_a$  [21], which embodies the actual performance of the ceramsite aggregate particle embedded in LWAC.

At normal temperature, the strength of ceramsite aggregates is weaker than that of hardened cement paste. The damage state

whether in compressive or splitting tensile loading typically characterizes the crack of most of ceramsite particles on the damage surface shown in Fig.1. This indicates that the ITZ is in relatively well performance, the collaboration between the coarse ceramsite aggregate and hardened mortar works well with effective bonding. As the temperature elevating, the dehydration of the primary hydration products in ITZ results in the performance degeneration of the ITZ and weakens the bonding. After 800°C high temperature, the damage characteristic changes clearly shown in Fig.1. Many ceramsite aggregate particles on the damage surface are intact whether in compressive or tensile loading state. The performance of ITZ and the hardened mortar weaken obviously. It directly leads to clear degeneration of the effective stiffness contribution of ceramsite aggregates to LWAC.

For the similar material properties both of fine and coarse aggregates in NWAC, Lee et al. synthetically considered the influence of fine and coarse aggregates together with the ITZ after high temperature, and a unified and combined thermal degeneration factor was suggested as following [7],

$$f'_{agg} = 0.03921 + e^{-0.002T} \quad (17)$$

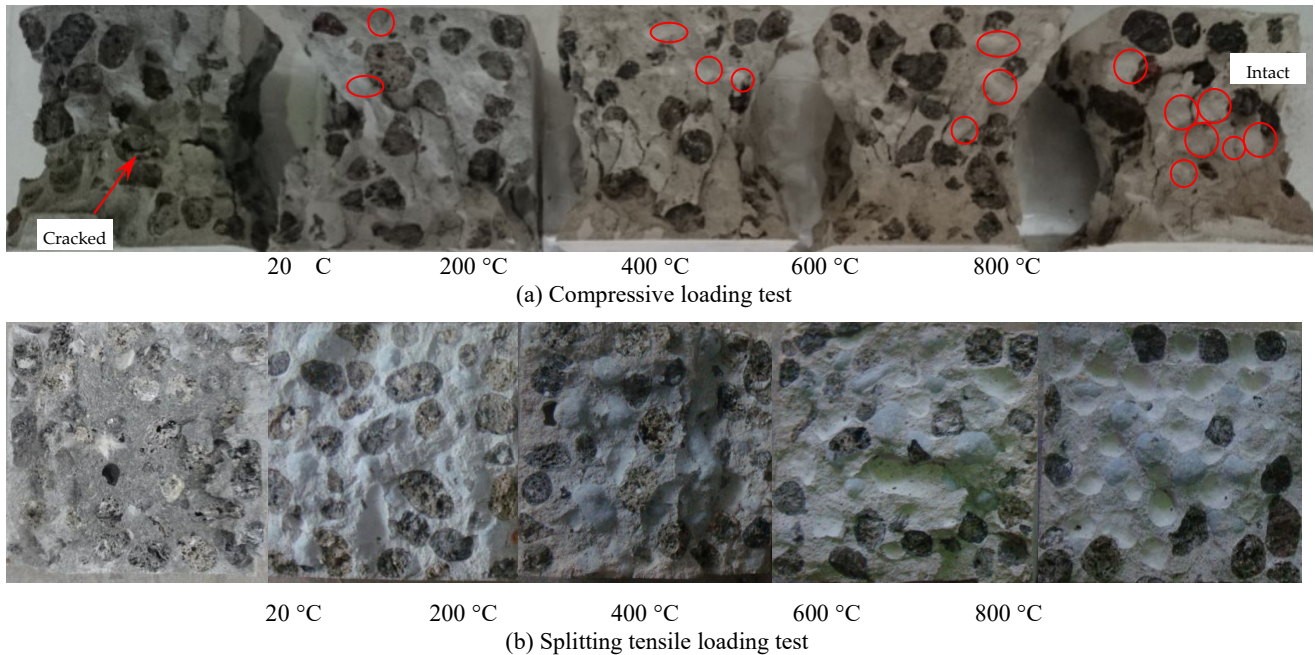


Fig. 1 - Characteristic on the damage surface after elevated temperatures.

However, clear difference exists in the mechanical performance and thermal degradation for ceramsite aggregates in LWAC compared with conventional coarse aggregate (CCA) such as granitic gravels in NWAC. Liu proposed the model for the nominal elastic modulus of a ceramsite particle as following [21],

$$E_a = 0.008\rho_a^2 \text{ (MPa)} \quad (18)$$

### 3.2. Degradation model at the mortar and concrete levels

For the clear difference on the mechanical and thermal performances of the fine aggregates such as sands and coarse ceramsite aggregates in LWAC,  $f_{agg}$  is introduced to represent the influence of fine aggregates and coarse ceramsite aggregates on the thermal degradation of the

$\rho_a$  is the apparent density of ceramsite aggregates. At the same time, the effective elastic modulus  $E'_a$  was proposed as following,

$$E'_a = 0.0106\rho_a^2 \text{ (MPa)} \quad (19)$$

Compared with  $E_a$  of a single ceramsite particle in Eq.(18),  $E'_a$  represents the real performance of ceramsite aggregates embedded in LWAC under loading. It synthetically reflects the particle shape effect of ceramsite aggregates, the performance of ITZ and real stress/strain state of ceramsite aggregates.

Considering the variation of the damage characteristic on the crack surface of the test blocks under loading after elevated temperatures, the effective stiffness contribution of ceramsite aggregates on LWAC under normal temperature can be represented by the effective elastic modulus  $E'_a$ . It is found in the test that not all ceramsite particles were cracked on the damage surface after 800°C; and the loading test above 800°C high temperature is not satisfactorily conducted for easy spalling happening. It is assumed in this paper that at 1000°C high temperature, the effective bonding performance of ITZ on ceramsite aggregates in LWAC completely disappears in the model. The actual stiffness contribution of ceramsite aggregates to LWAC is represented by the nominal elastic modulus  $E_a$ . The thermal degradation formula  $f'_{agg}$  of the ceramsite coarse aggregates in LWAC is expressed as following,

$$f'_{agg} = a + e^{b \times T} \quad (20)$$

where  $a$  and  $b$  are determined by inserting Eq.(18) and Eq.(19) into Eq.(20).

elastic modulus of LWAC after elevated temperatures. Based on Eq.(17), Eq.(20), the volume fraction of fine aggregates and coarse ceramsite aggregates in LWAC,  $f_{agg}$  is expressed as,

$$f_{agg} = \frac{f' \times f'_{agg} + f'' \times f''_{agg}}{f' + f''} \quad (21)$$

Finally, the thermal degradation model of elastic modulus of LWAC is formulated as,

$$E_e^T = \left( \prod_{j=C_{3.4}S_2H_3}^N f_j^T \right) f_{agg} \cdot E_{Ref} = F(T) \cdot E_{Ref} \quad (22)$$

#### 4. Results comparison and discussion

The stiffness of each constituent paste can be obtained from the expressions to formulate the degradation model of the elastic modulus of LWAC after elevated temperatures [22]. Table 6 gives a summary of the elastic modulus of each phase used in the present model.  $p_i$  denotes the porosity of each decomposed phase, which affects the elastic modulus of  $C_{3.4}S_2$  and CaO decomposed from  $C_{3.4}S_2H_3$  and CH respectively. The proposed degradation model of the elastic modulus for LWAC are determined according to Eq.(15) and Eq.(22) as,

$$F(T) = (-4.567e^{-4} + e^{-5.798e^{-4}T}) \quad (20^\circ C \leq T < 120^\circ C) \quad (23)$$

$$F(T) = (-4.567e^{-4} + e^{-5.798e^{-4}T})(0.0826 + e^{-0.0007T}) \quad (120^\circ C \leq T < 400^\circ C) \quad (24)$$

$$F(T) = (-4.567e^{-4} + e^{-5.798e^{-4}T})(0.0826 + e^{-0.0007T})(2.926 - 4.815e^{-3}T) \quad (400^\circ C \leq T < 530^\circ C) \quad (25)$$

$$F(T) = 0.374(-4.567e^{-4} + e^{-5.798e^{-4}T})(0.0826 + e^{-0.0007T}) \quad (530^\circ C \leq T < 800^\circ C) \quad (26)$$

Table 6

Elastic moduli of each constituent phase		
Phases	$p_i$ (porosity)	$E$ (Gpa)
$C_{3.4}S_2H_3$	-	32.0
$C_{3.4}S_2$	0.26	29.79 (from $E = 120(1 - p_{C_{3.4}S_2})^n, n = 4.65$ )
CH	-	40.2
CaO	0.54	8.35 (from $E = 194.54(1 - p_{CaO})^n, n = 4$ )
Void	-	0

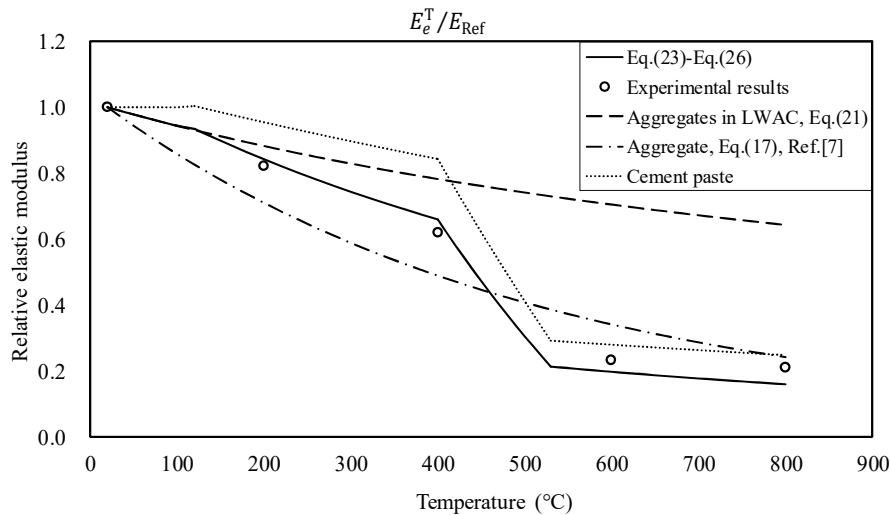


Fig. 2 - The relationship between relative elastic modulus and temperatures of proposed model and experimental results

Due to the different phase transformations occurring during different high temperature ranges, the final degradation formulas is expressed as a polyline model. It denotes the normalized ratios of the residual elastic modulus of LWAC to the original ones after elevated temperatures. The presented degradation model for the elastic modulus of LWAC is compared with the experimental results shown in Fig.2, in which the experimental results are the average of three batches test blocks.

(1) The model-based results are consistent with the experimental values with regarding to the elevated temperatures. After 200°C and 400°C temperatures, the experimental results are a little lower than that from the presented model. The possible reason might be there is no consideration on the emergence of micro- and meso-cracks in LWAC in the presented model. The experimental phenomenon shows there are obvious cracks generated on the surface of test blocks after 200°C temperature.

(2) Comparatively, the experimental results at 600°C and 800°C elevated temperatures are a little higher than that of the presented model. It might be a little underestimated by using the nominal elastic modulus of ceramsite particle to represent the actual stiffness of ceramsite aggregates LWAC at 1000°C.

(3) Eq.(17) synthetically considers the effect of all aggregates on stiffness of NWAC, in which all aggregates are similar materials. With the increase of temperature, the performance of ceramsite aggregates is definitely different from CCA. As the temperature increases, the internal stress of LWAC is effectively reduced and the deterioration of ITZ is lightened. Therefore, the reduction of the synthetic effect of ceramsite aggregates on stiffness of LWAC is less than that of CCA in NWAC as temperature rises, which is shown in Fig.2.

## 5. Conclusions

The performance of ceramsite aggregates in LWAC is distinctive compared with the normal coarse aggregates in NWAC at high temperatures. Considering the change law of the LWAC damage characteristic after elevated temperatures, a degradation model of the elastic modulus is proposed. The effective elastic modulus  $E_a$  of ceramsite aggregates embedded in LWAC and the nominal elastic modulus  $E_a$  of ceramsite particles are utilized to formulate the degradation for the stiffness contribution of ceramsite aggregates to LWAC with regarding to elevated temperatures. (1) The degradation model for the elastic modulus of LWAC can't be expressed by a continuous function curve because different phase transformation processes occur during different temperature ranges; (2) The influence of ceramsite aggregates on the elastic modulus of LWAC should be considered independent of fine aggregates such as ordinary sands, because clear differences exist in the thermal performance between ceramsite aggregates and sands; (3) The consistence between the presented model and experimental results indicates the effectiveness of the proposed formula on the stiffness influence of ceramsite aggregates to LWAC after elevated temperatures.

## Acknowledgements

This work was supported by National Natural Science Foundation of China [No. 51878360, No. 51778302] and Natural Science Foundation of Zhejiang Province [LY18E080008].

REFERENCES

- [1] P. Wriggers, S.O. Mofteh. Mesoscale models for concrete: Homogenization and damage behavior. *Finite Elements in Analysis and Design*, 2006, **42**(7), 623-636.
- [2] G. Constantinides, F.J. Ulm. The effect of two types of C-S-H on the elasticity of cement-based materials: results from nanoindentation and micromechanical modeling. *Cement and Concrete Research*, 2004, **34** (11), 67–80.
- [3] K.J. Mun. Development and tests of lightweight aggregate using sewage sludge for nonstructural concrete. *Construction and Building Materials*, 2007, **21**(7):1583–1588.
- [4] A.M. Neville. *Properties of concrete*. 4th edition. Longman, 1995.
- [5] F.K. Kong, R.H. Evans, E. Cohen, F. Roll. *Handbook of structural concrete*. London: Pitman Books Limited, 1983.
- [6] P.W. Abeles, B.K. Bardhan-Roy. *Prestressed concrete designer's handbook*. Cement and concrete association, Wexham Springs: A View point Publication; 1981.
- [7] J. Lee, Y. Xi, K. Willam, Y. Jung. A multiscale model for modulus of elasticity of concrete at high temperatures. *Cement and Concrete Research*, 2009, **39**(9), 754–762.
- [8] H. Chen, T. Yen, K. Chen. Evaluating elastic modulus of lightweight aggregate. *ACI Materials Journal*, 2003, **100**(2), 108–113.
- [9] P.B. Bamforth. The properties of high strength lightweight concrete. *Concrete*, 1987, **2**, 8–9.
- [10] O. Bernard, F.J. Ulm, E. Lemarchand. A multiscale micromechanics-hydration model for the early-age elastic properties of cement-based materials. *Cement and Concrete Research*, 2003, **33** (9), 1293–1309.
- [11] D.P. Benz. Influence of water-to-cement ratio on hydration kinetics: Simple models based on spatial considerations. *Cement and Concrete Research*, 2006, **36** (2), 238-244.
- [12] V. Zanjani Zadeh, C. Bobko. Nanomechanical characteristics of lightweight aggregate concrete containing supplementary cementitious materials exposed to elevated temperature. *Construction and Building Materials*, 2014, **51**, 198–206.
- [13] J. Formosa, JM. Chimenos, AM. Lacasta, L. Haurie, JR. Rosell. Novel fire-protecting mortars formulated with magnesium by-products. *Cement and Concrete Research*, 2011, **41**(2),191-196.
- [14] B. Demirel, O. Kelestemur. Effect of elevated temperature on the mechanical properties of concrete produced with finely ground pumice and silica fume. *Fire Safety Journal*, 2010, **45**(6), 385-391.
- [15] M.A. Othuman, Y.C. Wang. Elevated-temperature thermal properties of lightweight foamed concrete. *Construction and Building Materials*, 2011, **25**(2), 705-716.
- [16] L.E. Copeland, R.H. Bragg. The determination of non-evaporable water in hardened Portland cement paste. *ASTM Bulletin*, ASTM, Philadelphia, 1953, **194**, 70-74.
- [17] P.D. Tennis, H.M. Jennings. A model for two types of calcium silicate hydrate in the microstructure of Portland cement pastes. *Cement and Concrete Research*, 2000, **30**(6), 855-863.
- [18] J. Piasta, Z. Sawicz, L. Rudzinski. Changes in the structure of hardened cement paste due to high temperature. *Materials and Constructions*, 1984, **17**(4), 291-296.
- [19] Y. Xi, A. Nakhi. Composite damage models for diffusivity of distressed materials. *Journal of Materials in Civil Engineering*, ASCE, 2005, **17** (3), 286–295.
- [20] Y. Xi, M. Eskandari-Ghadi, Suwito, S. Sture. Damage theory based on composite mechanics. *Journal of Engineering Mechanics*, ASCE, 2006, **132** (11), 1195–1204.
- [21] X.B. Liu, P.J. Li, Y.Q. Ji. The effective elastic modulus of ceramsite and its predication. *Concrete*, 2005, (3): 35–38. (In Chinese).
- [22] K. Velez, S. Maximilien, D. Damidot, G. Fantozzi, F. Sorrentino. Determination by nanoindentation of elastic modulus and hardness of pure constituents of Portland cement clinker. *Cement and Concrete Research*, 2001, **31** (4), 555–561.

\*\*\*\*\*